Supporting information

In vitro assembly of diverse bacterial microcompartment shell architectures

Andrew R. Hagen[a], Jefferson S. Plegaria[b], Nancy Sloan[a], Bryan Ferlez[b], Clement Aussignargues[a], and Cheryl A. Kerfeld[a,b,c]*

[a]Environmental Genomics and Systems Biology and Molecular Biophysics and Integrated Bioimaging Divisions, Lawrence Berkeley National Laboratory, 1 Cyclotron Road Berkeley, CA 94720, USA

[b]MSU-DOE Plant Research Laboratory, Michigan State University, 612 Wilson Road East Lansing, MI 48824, USA

[c]Department of Biochemistry and Molecular Biology, Michigan State University, 603 Wilson Road East Lansing, MI 48824, USA

*Corresponding Author: Cheryl A. Kerfeld (ckerfeld@lbl.gov)

Materials and Methods

Chemicals and Reagents

Lipoic acid-capped gold nanoparticles (diameter = 5 nm) made by Nanocomposix were purchased from Fischer Scientific (Hampton, NH), all other chemicals were purchased from Millipore-Sigma (St. Louis, USA).

Protein expression and purifications

All protein expressions were performed in *E. coli* BL21(DE3). Strains were cultured in lysogeny broth (LB) and induced at mid-log with either with 20-50 ng/ml anhydrotetracycline (aTc; E2k-based plasmids) or 50 uM Isopropyl β-D-1-thiogalactopyranoside (IPTG; pET-based plasmids). Cell pellets were resuspended in their respective column's equilibration buffer (4 ml buffer per gram cell paste) with the addition of a few crystals of hen egg lysozyme and DNase and lysed by french press. Crude lysates were clarified by centrifugation at 25,000 x g for 30 minutes and supernatants removed to clean tubes. Column chromatography was performed using an Äkta Pure chromatography system (GE Healthcare) except for StrepTrap purifications which were performed with a syringe pump. Protein concentrations were quantified via the Pierce™ BCA Protein Assay Kit using bovine serum albumin in comparable buffers for creation of standard curves.

In vitro assembly set ups and shell isolation with CAP

In vitro assembly reactions were set up using 10-15 µM total final target concentration of cleaved hexamer subunit(s) (e.g. BMC-H_{HO}, BMC-H_{ccmK1} + BMC-H_{ccmK2}) and stoichiometric amounts (when

known) of other subunits in TBS 50/150 pH 7.4, 5% glycerol, 1 mM TCEP and 1 mM EDTA. To remove the SUMO domain, MBP-Ulp was added to an amount corresponding to 1:20 of the SUMOylated protein(s) (mass basis). For HO shells, assuming 100% cleavage and assembly efficiencies and a 60:20:12 stoichiometry between hexamer, trimer and pentamer subunits, final theoretical shell particle concentrations are 166-200 nM. The Halo shell assembly reaction had a 6:1:1 ratio between hexamer, trimer and pentamer subunits, respectively. While care was taken to have identical buffer conditions for all reactions, salt carry-over from certain protein preparations caused deviations in sodium chloride concentrations of no more than 15% in some reactions with no apparent impact on assembly.

Where noted, assembled shells were isolated from unassembled proteins in reactions via complementation-based affinity chromatography (CAP) (**Hagen 2018**). Briefly, reactions were diluted to 5 ml with **Buffer 1** (100 mM Tris-HCl pH 8.0, 150 mM NaCl, 1 mM EDTA) for ease of handling and applied to a 1 ml StrepTrap column (GE Healthcare). Columns were then washed with 5 ml **Buffer 1** and eluted with 5 ml **Buffer 1** supplemented with 2.5 mM *d*-desthiobiotin (Millipore-Sigma, St. Louis).

The encapsulation experiments were performed with either 3x RraB-GFP/GFP or 0.1x AuCOOH with respect to the $_{SUMO}$BMC-H$_{HO}$ concentration. These reactions were purified using Strep-Tactin XT Spin columns (IBA-Lifesciences). Purifications were performed as described in the company's protocol. Shells were eluted in **Buffer 1** (without EDTA) containing 50 mM *d*-biotin (IBA-Lifesciences).

In vitro assembly of BMC-H$_{Rmm}$ nanotubes

In vitro assembly reactions were set up using 40 mg/ml $_{SUMO}$BMC-H$_{Rmm}$ (final concentration) in TBS 50/50 pH 8.0, 0.2% IGEPAL, and 1 mM DTT. MBP-Ulp was added to an amount corresponding to 1:20 of the SUMOylated protein (mass basis) and the assembly reaction was incubated at room temperature overnight.

SDS-PAGE analysis of assembly and shell yield; TCA precipitation

Samples were heat-denatured in reducing SDS-PAGE sample buffer and resolved with 4–20% Mini-PROTEAN® TGX™ precast protein gels (Bio-Rad, Hercules USA). Where stated, samples were concentrated via trichloroacetic acid (TCA) precipitation. Briefly, 250 µl concentrated TCA was added to 1 ml of eluate and incubated on ice for 1 h. Precipitated protein was pelleted at 20,000 x g for 30 minutes and the pellet washed with 100% cold acetone. 20 µl of 8 M urea was used to dissolve the pellet (now 50x concentrated) which was then diluted appropriately prior to denaturation and electrophoresis.

The GFP encapsulation experiments were heat-denatured in reducing SDS-PAGE sample buffer and resolved with 16% homemade protein gels. These samples were not concentrated via TCA precipitation. Twenty µl of samples were loaded in all the lanes containing 1.2 – 1.9 µg of protein.

TEM analysis

For *in vitro* assembly reactions of HO and Halo shells, 6 µl of the neat reactions were mounted on formvar/carbon-coated copper grids (Electron Microscopy Sciences, No. 456 FCF300-Cu) for 30 seconds and then wicked away with filter paper. The grids were washed three times in 6 µl drops of water, dried with filter paper and then negatively stained with 5 µl 1% (w/v) aqueous uranyl acetate or

ammonium molybdate. After ten seconds, the stain was wicked off and the grids allowed to dry. Images were taken on a Tecnai 12 TEM operated at an accelerating voltage of 120 kV using an Ultrascan 1000 2k x 2k CCD camera.

For mHO^{+}/mHO shells assembled in the presence of AuCOOH or (±RraB-) GFP, 5 µl of a purified reaction or a ten-fold dilution in HPLC-grade water were mounted on carbon-coated copper grids (Electron Microscopy Sciences, CF150-Cu) for 30 seconds. For BMC-H_{Rmm} nanotubes, 5 µl of a 20-fold dilution in HPLC-grade water of the neat *in vitro* assembly reaction was mounted on carbon-coated grids for 30 seconds. Grids were wicked dry and stained with 5 µl 1% (w/v) aqueous uranyl acetate or ammonium molybdate for 15 seconds. Grids were again wicked dry and imaged using a JEOL 100CXII operated at an accelerating voltage of 100 kV using a Gatan Orius SC200 CCD camera.

The diameters of the shells in the TEM images were measured using the ImageJ software. The diameter of 70 – 100 shells were measured and averaged.

TEM thin section analysis

BL21(DE3) cells induced with 450 µM IPTG at 37 C for 4 h (typically 10 ml) were pelleted, resuspended in 1.4 ml of fixation buffer (100 mM sodium cacodylate pH 7.4 containing formaldehyde/glutaraldehyde (3% v/v)) and then incubated overnight at 4 C with gentle shaking. After centrifugation, the cell pellets were embedded in 2% agarose, washed four times (5 min each) with 100 mM sodium cacodylate pH 7.4, and post-fixed in 1% (w/v) osmium tetroxide and 1.6% (w/v) potassium ferricyanide in 100 mM sodium cacodylate pH 7.4 for 2 h at room temperature. The samples were washed five times with ddH_2O (ten min each) and dehydrated using a gradient of acetone (5-10 min incubation in 30, 50, 70, 80, 90, 95, 100% v/v; the 100% step was repeated three times). Infiltration in Spurr resin was performed by incubating for 8 h-overnight in increasing concentrations of resin diluted in acetone (25, 50, 75, 100 % v/v resin; the 100% step was repeated three times). The samples were deposited in an open mold and embedded in fresh resin. Polymerization was achieved after 48 h of incubation at 60 C. 50-70 nm thin sections obtained using a Power Tome Ultramicrotome (RMC, Boeckeler Instruments. Tucson, AZ) with a diamond knife (Diatome 45°) were collected on uncoated 300 mesh copper grids. Post-staining was performed with 4% (w/v) uranyl acetate in ddH_2O for 25 min followed by a wash with ddH_2O, incubation with Reynolds lead citrate for 20 min and a final wash with ddH_2O. Imaging was performed using a JEOL 100CXII operated at an accelerating voltage of 100 kV using a Gatan Orius SC200 CCD camera.

Fluorescence analysis

Emission spectra were recorded at room temperature using a SpectraMax M2 (Molecular Devices) fluorimeter. mHO + GFP eluates were excited at 495 nm and fluorescence emission spectra were recorded from 500 to 600 nm. Each *in vitro* encapsulation reaction was completed in triplicate using separately purified samples using the Strep-Tactin XT Spin column. The eluates contained 0.15 – 0.46 mg/mL total protein content.

UV-transilluminator images were collected on a Bio-Rad ChemiDoc MP imager using a 530 nm filter with a bandwidth of 28 nm (Bio-Rad, Hercules USA).

DLS analysis

Experiments were performed on a Dynapro (Wyatt Technologies) with 20 acquisitions of 5 s each, at room temperature. DLS histograms were collected on the purification eluates in **Buffer 1**, containing either *d*-desthiobiotin or *d*-biotin.

Protein expression/purification details

$_{SUMO}$BMC-H$_{HO}$ (Ho5815):

Expressed from plasmid pARH226 at 2 L scale and cultured at 37 C for 4-6 h post-induction. Clarified lysates were applied to a 5 ml HisTrap column (GE Healthcare) equilibrated with **Buffer A** (20 mM Tris-HCl pH 7.6, 300 mM NaCl and 20 mM imidazole). The column was washed until the A280 returned to baseline and the protein was then eluted over a ten column volume gradient to 100% **Buffer B** (20 mM Tris-HCl pH 7.6, 300 mM NaCl and 500 mM imidazole). Fractions containing the target protein (as determined by SDS-PAGE) were pooled then concentrated and exchanged into **Buffer C** (20 mM Tris-HCl pH 7.6, 500 mM NaCl) with a 100 kDa MWCO spin filter (Amicon). Glycerol was then added to a final percentage of 10% and small aliquots of protein were flash frozen in liquid nitrogen for storage.

BMC-T1$_{HO}$ (Ho5812):

Expressed from plasmid pCA14[1] at 4 L scale and cultured at 18 C overnight post-induction.[1] HiTrap anion exchange purification was performed, as previously described. Protein was then concentrated with a fresh 30 kDa MWCO spin filter, followed by addition of glycerol and snap freezing as described for $_{SUMO}$BMC-H$_{HO}$.

BMC-P$_{SIIHO}$: (Ho5814$_{SII}$):

Purified as previously described.[2] Briefly, cultures expressed from plasmid pARH292 were purified by application to a 5 ml StrepTrap column (GE healthcare) according to manufacturer's recommendations and polished via application to a MonoQ anion-exchange column. Eluates were concentrated and buffer exchanged into **Buffer C** with 30 kDa MWCO spin filters, followed by addition of glycerol and snap freezing as described.

$_{SUMO}$BMC-H$_{ccmK1}$ (ccmK1), $_{SUMO}$BMC-H$_{ccmK2}$ (ccmK2) and BMC-T$_{ccmO}$ (ccmO):

Expressed from plasmids pARH284, pARH285 and pET45b::ccmO, respectively at 1-2 L scale and cultured at 37 C for 4-6 h post-induction. Proteins were purified, buffer-exchanged and snap-frozen as was done for $_{SUMO}$BMC-H$_{HO}$.

BMC-P$_{SIIccmL}$ (ccmL):

Expressed from plasmid pARH412 at 2 L scale and cultured at 18 C overnight post-induction. Protein was purified, buffer exchanged and snap-frozen as with BMC-P$_{SIIHO}$ except no MonoQ polishing step was performed.

$_{SUMO}$BMC-H$_{Rmm}$ (RmmH):

Expressed from plasmid pRB1 at 2 L scale and cultured at 37 C for 4-6 h post-induction. HisTrap purifications were performed as for $_{SUMO}$BMC-H$_{HO}$. Eluate was exchanged into 20 mM Tris-HCl pH 7.6, 100 mM NaCl and further purified with a Superdex 200 size exclusion column (GE healthcare).

Pooled eluate was exchanged into **Buffer C** (20 mM Tris-HCl pH 7.6, 500 mM NaCl) using a Sephadex (PD10) desalting column (GE Healthcare). Ten percent glycerol and 0.02% NaN_3 were then added before storing at -80 C.

SUMO Protease ($_{6xHis}$MBPtev-Ulp403-621):
The SUMO protease was expressed and purified separately as a hexahistidine-tagged maltose-binding protein[3] (MBP-Ulp) fusion. Fusion of MBP to Ulp promoted soluble expression of the protease, provided a convenient affinity handle for purification, and increased the molecular weight of the protein so that the fusion could be easily discriminated from shell proteins in complex samples. MBP-Ulp was expressed from plasmid pARH236 at 4 L scale and cultured at 18 C overnight post-induction. HisTrap purification and polishing via MonoQ was performed as described. Eluates were exchanged into **Buffer D** (20 mM Tris-HCl pH 7.6, 200 mM NaCl, 1 mM TCEP, 0.02% NaN_3) via spin-dialysis, one volume of 100% glycerol was added and the preparation stored at -20 C.

$_{SUMO}$BMC-H^+_{HO} (Ho5815_E65R_E69R):
Expressed from plasmid pCF1 at 4 L scale and cultured at 37 C for 4-6 h post-induction. HisTrap purification was performed as described for $_{SUMO}$BMC-H_{HO}. Eluates were exchanged into **Buffer C** (20 mM Tris-HCl pH 7.6, 500 mM NaCl) using a Sephadex (PD10) desalting column (GE Healthcare). Ten percent glycerol and 0.02% NaN_3 were then added before storing at -80 C.

RraB-GFP and GFP:
RraB-GFP and GFP were expressed from plasmid pBF46 and pBF55, respectively, at 2 L scale and cultured at 22 C overnight post-induction. HisTrap purification was performed as described for $_{SUMO}$BMC-H_{HO}^+. Eluates were exchanged into **Buffer C** (20 mM Tris-HCl pH 7.6, 500 mM NaCl) using a Sephadex (PD10) desalting column (GE Healthcare). Ten percent glycerol and 0.02% NaN_3 were then added before storing at -80 C.

Molecular Modeling
UCSF Chimera and PyMol (The PyMOL Molecular Graphics System, Version 2.0 Schrödinger, LLC.) were used for molecular visualizations and figure creation. To create the $_{SUMO}$BMC-H_{HO} model, the original atomic coordinates of the SUMO domain (PDB ID: 1EUV) and BMC-H_{HO} (PDB ID: 5DJB) were retrieved. One protomer of the BMC-H hexamer was then appended to the end of the SUMO domain using the join model command in Chimera. This model was imported into FoldIt and allowed to minimize through side-chain and backbone “wiggling” of the interdomain junction. The minimized $_{SUMO}$BMC-H_{HO} protomer was then hexamerized using match commands to the original BMC-H_{HO} model.

Plasmid Construction and notes

Alias	Plasmid identity
pARH236	pBbE2k::$_{6xHis}$MBPtev-Ulp403-621

A truncated version of the 621 amino acid Ulp1 protein from *S. cerevisiae* corresponding to its protease domain [Ulp1(403-621)][4] was codon-optimized for *E. coli* and ligated into a high-copy variant of pARH098[14] using NdeI/XhoI sites

pARH226 pBbE2k::$_{6xHis}$SUMO-Ho5815

Using *S. cerevisiae*'s Smt3 ORF as the SUMO domain, a $_{6xHis}$SUMO-Ho5815 fusion was codon-optimized for *E. coli* and ligated into the pBbE2k vector[5] using flanking NdeI/BamHI sites.

pET11b::Ho5815
Previously described.[6]

pARH284 pBbE2k::$_{6xHis}$SUMO-K1_Halo
pARH285 pBbE2k::$_{6xHis}$SUMO-K2_Halo
pRB1 pBbE2k::$_{6xHis}$SUMO-RmmH_Msme
All above SUMOylated constructs were created using Gibson assemblies wherein fusion targets (RmmH, K1 etc.) were PCR amplified with the required homology arms and used to replace Ho5815 in combination with generic pBbE2k::$_{6xHis}$SUMO vector pieces.

pARH292 pBbE2k::Ho5814$_{SII}$
As previously described.[2]

pCF1 pBbE2k::$_{6xHis}$SUMO-Ho5815_E65R, E69R
This plasmid was created via the QuikChange Lightning Site-Directed Mutagenesis Kit, using pARH226 as the template plasmid.

pBF46 pACYCDUET-1:: Rrab-sfGFP$_{6xHis}$
The gene for RraB[7, 8]-superfolderGFP[9] (sfGFP), which has a (3x) GlySer linker between the two domains and a C-terminal polyhistidine tag (GlySer-6xHis), fusion construct was synthesized by Integrated DNA Technologies using *Escherichia coli* codon optimization. This gene was cloned into the pACYCDuet-1 vector (Novagen) using NcoI and NotI sites.

pBF55 pACYCDUET-1::sfGFP$_{6XHis}$
This plasmid was prepared by removing the rraB gene and sequence encoding the (3x) GlySer linker from pBF46 via Gibson Assembly.

pCA14 pET11b::Ho5812
Previously described.[1]

Protein sequences of engineered proteins

$_{6xHis}$MBPtev-Ulp403-621	MHHHHHHSSGKIEEGKLVIWINGDKGYNGLAEVGKKFEKDTGIKVTVEHPDKLEEKFP QVAATGDGPDIIFWAHDRFGGYAQSGLLAEITPDKAFQDKLYPFTWDAVRYNGKLIAY PIAVEALSLIYNKDLLPNPPKTWEEIPALDKELKAKGKSALMFNLQEPYFTWPLIAADG GYAFKYENGKYDIKDVGVDNAGAKAGLTFLVDLIKNKHMNADTDYSIAEAAFNKGETA MTINGPWAWSNIDTSKVNYGVTVLPTFKGQPSKPFVGVLSAGINAASPNKELAKEFLE NYLLTDEGLEAVNKDKPLGAVALKSYEEELAKDPRIAATMENAQKGEIMPNIPQMSAF WYAVRTAVINAASGRQTVDEALKDAQTDYDIPTTENLYFQGHMLVPELNEKDDDQVQ KALASRENTQLMNRDNIEITVRDFKTLAPRRWLNDTIIEFFMKYIEKSTPNTVAFNSFFY TNLSERGYQGVRRWMKRKKTQIDKLDKIFTPINLNQSHWALGIIDLKKKTIGYVDSLSN GPNAMSFAILTDLQKYVMEESKHTIGEDFDLIHLDCPQQPNGYDCGIYVCMNTLYGSA DAPLDFDYKDAIRMRRFIAHLILTDALKLE
6xHisSUMO domain	MGSSHHHHHHGSGLVPRGSASMSDSEVNQEAKPEVKPEVKPETHINLKVSDGSSEIF FKIKKTTPLRRLMEAFAKRQGKEMDSLRFLYDGIRIQADQTPEDLDMEDNDIIEAHREQ IGG

$_{SUMO}$BMC-H$_{HO}$	**(6xHisSUMO)**MADALGMIEVRGFVGMVEAADAMVKAAKVELIGYEKTGGGYVTAVVR GDVAAVKAATEAGQRAAERVGEVVAVHVIPRPHVNVDAALPLGRTPGMDKSA
$_{SUMO}$BMC-H$_{ccmK1}$	**(6xHisSUMO)**MAVAVGMIETLGFPAVVEAADAMVKAARVTLVGYEKIGTGRVTVIVRG DVSEVQASVSAGTESVKRVNGGQVLSTHIIARPHENLEYVLPIRYTEEVEQFREGVGT PRNITRQ
$_{SUMO}$BMC-H$_{ccmK2}$	**(6xHisSUMO)**MPIAVGMIETLGFPAVVEAADAMVKAARVTLVGYEKIGTGRVTVIVRGD VSEVQASVSAGVDSANRVNGGEVLSTHIIARPHENLEYVLPIRYTEAVEQFR
$_{SUMO}$BMC-H$_{RmmH}$	**(6xHisSUMO)**MSSNAIGLIETKGYVAALAAADAMVKAANVTITDRQQVGDGLVAVIVTG EVGAVKAATEAGAETASQVGELVSVHVIPRPHSELGAHFSVSSK
$_{SUMO}$BMC-H$^{+}_{HO}$	**(6xHisSUMO)**MADALGMIEVRGFVGMVEAADAMVKAAKVELIGYEKTGGGYVTAVVR GDVAAVKAATEAGQRAA**R**RVG**R**VVAVHVIPRPHVNVDAALPLGRTPGMDKSA
Rrab-sfGFP$_{6xHis}$	MGSEQLEEQREETRLIIEELLEDGSDPDALYTIEHHLSADDLETLEKAAVEAFKLGYEV TDPEELEVEDGDIVICCDILSECALNADLIDAQVEQLMTLAEKFDVEYDGWGTYFEDP NGEDGDDEDFVDEDDDGSGSGSKGEELFTGVVPILVELDGDVNGHKFSVRGEGEGD ATNGKLTLKFICTTGKLPVPWPTLVTTLTYGVQCFARYPDHMKQHDFFKSAMPEGYV QERTISFKDDGTYKTRAEVKFEGDTLVNRIELKGIDFKEDGNILGHKLEYNFNSHNVYI TADKQKNGIKANFKIRHNVEDGSVQLADHYQQNTPIGDGPVLLPDNHYLSTQSVLSKD PNEKRDHMVLLEFVTAAGITHGMDELYKGSHHHHHH

Supplementary figures

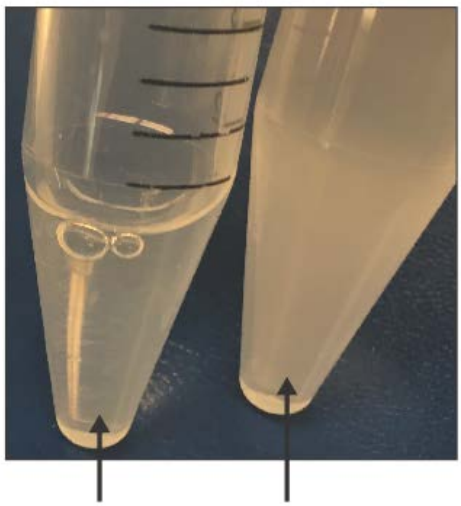

Figure S1. Purified $_{SUMO}$BMC-H$_{HO}$ behavior in high and low NaCl. Photograph depicting $_{SUMO}$BMC-H$_{HO}$ in high-salt HisTrap elution buffer (left) and upon buffer exchange into low-salt Tris-buffered saline (right). Note turbid appearance in low-salt buffer.

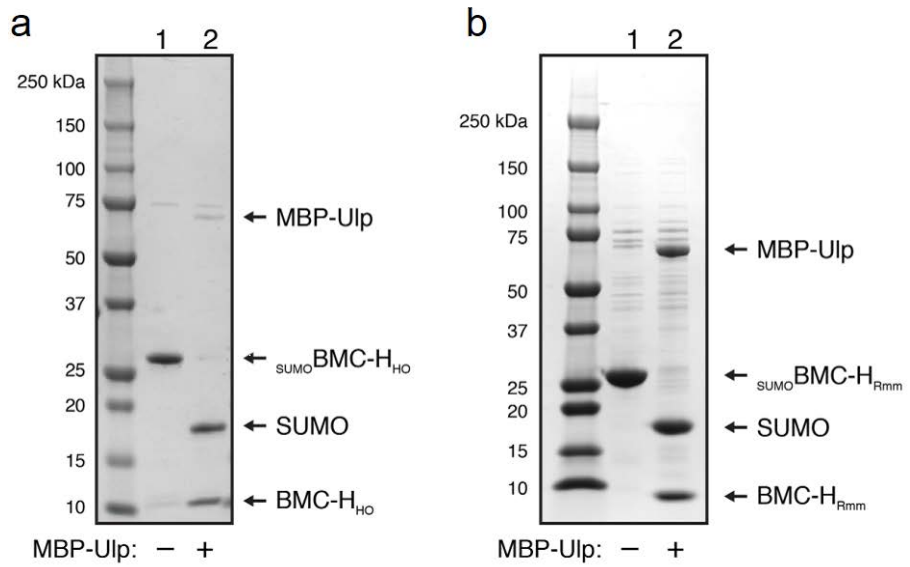

Figure S2. SDS-PAGE analysis of purified $_{SUMO}$BMC-H (lane 1) and its cleavage products (lane 2) after 1 h incubation with the SUMO protease. (a) $_{SUMO}$BMC-H$_{HO}$. (b) $_{SUMO}$BMC-H$_{Rmm}$.

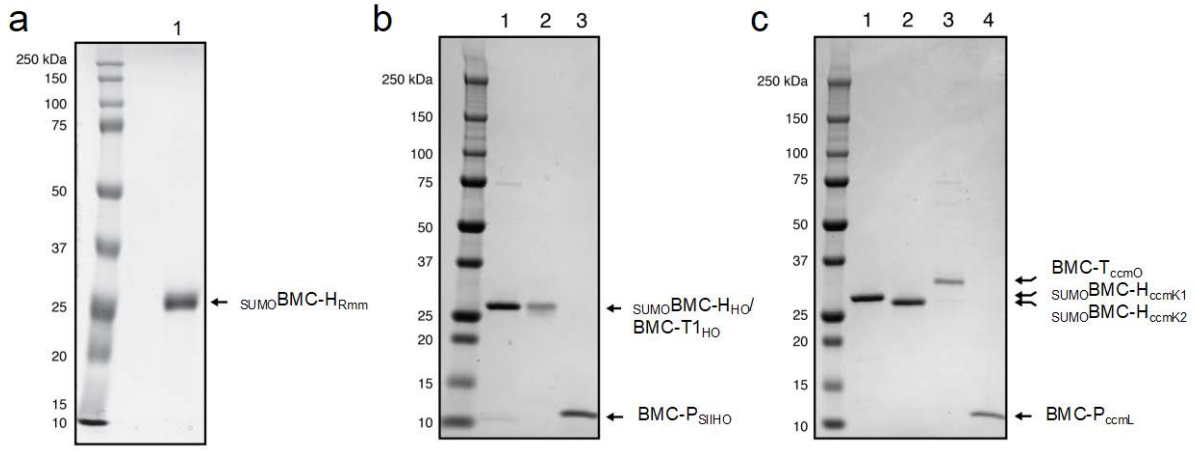

Figure S3. SDS-PAGE analysis of protein preps used for IV assemblies. (a) Lane 1: $_{SUMO}$BMC-H$_{RMM}$. (b) HO shell protein preparations. Lane 1: $_{SUMO}$BMC-H$_{HO}$, Lane 2: BMC-T1$_{HO}$, and Lane 3: BMC-P$_{SIIHO}$. (c) Halo shell protein preparations. Lane 1: $_{SUMO}$BMC-H$_{ccmK1}$, Lane 2: $_{SUMO}$BMC-H$_{ccmK2}$, Lane 3: BMC-T$_{ccmO}$, Lane 4: BMC-P$_{SIIccmL}$.

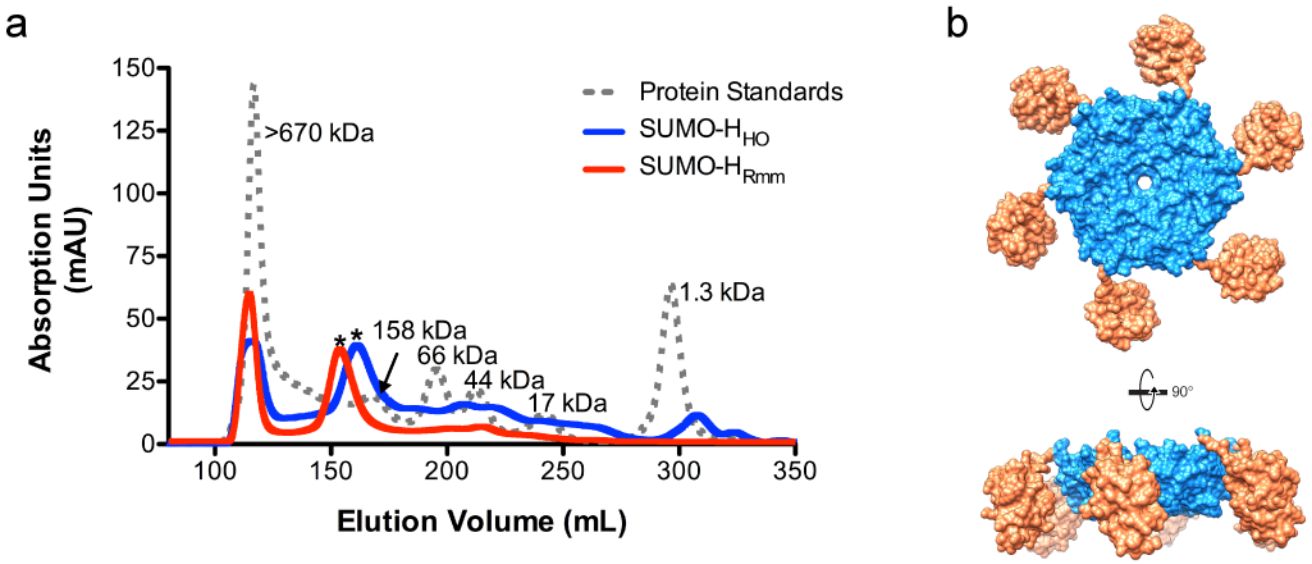

Figure S4. Size Exclusion Chromatography analysis and molecular model of $_{SUMO}$BMC-H proteins. (a) Chromatogram of $_{SUMO}$BMC-H$_{HO}$ and $_{SUMO}$BMC-H$_{RMM}$ including size standards. Major peaks corresponding to approximate size of hexameric species (141 kDa and 136 kDa theoretical mass for $_{SUMO}$BMC-H$_{HO}$ and $_{SUMO}$BMC-H$_{RMM}$, respectively) are indicated with asterisks. (b) Molecular surface model of $_{SUMO}$BMC-H$_{HO}$ with SUMO domains rendered in coral and BMC-H domains in blue.

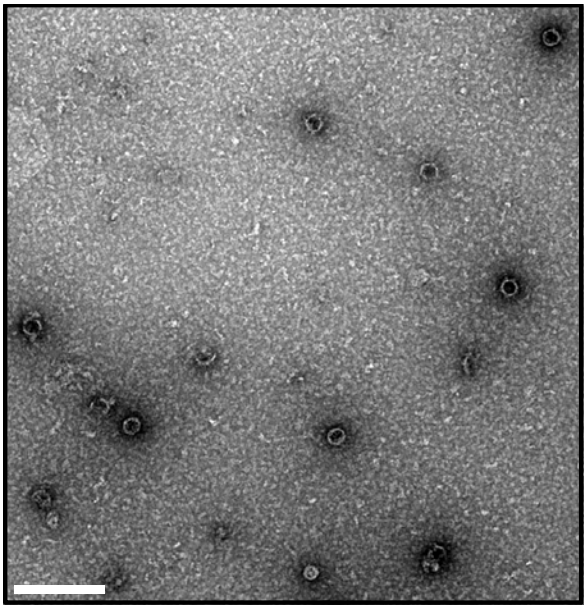

Figure S5. TEM analysis of *in vitro* minimal HO shell assembly reaction without MBP-Ulp. Scale bar = 200 nm.

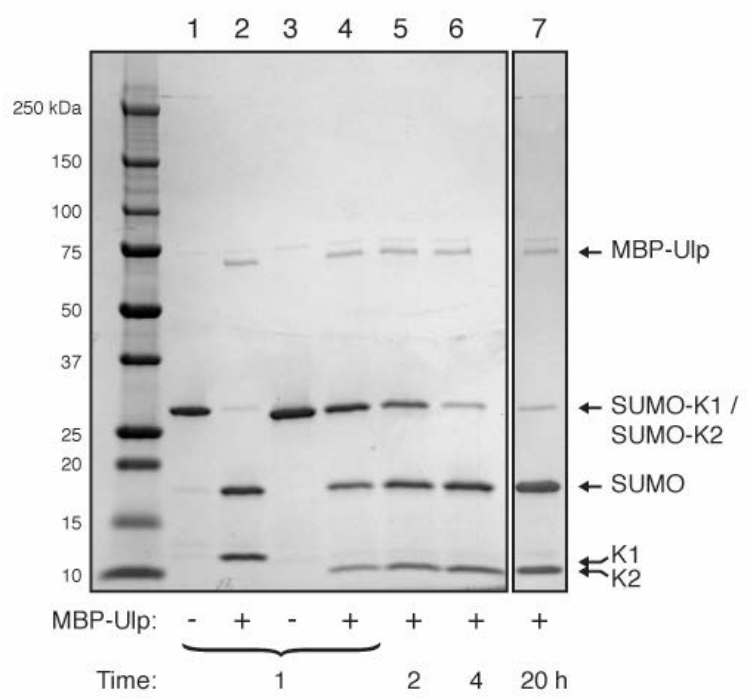

Figure S6. Cleavage behavior of SUMOylated Halo hexamers. Halo proteins: $_{SUMO}$BMC-H$_{ccmK1}$ (lane 1) and its cleavage products (lane 2); $_{SUMO}$BMC-H$_{ccmK2}$ (lane 3) and its cleavage products after 1 h (lane 4), 2 h (lane 5), 4 h (lane 6) and 20 h (lane 7). The 20 h cleavage (lane 7) appears separate as this sample was generated and run on a different day (using identical proteins and reaction set up).

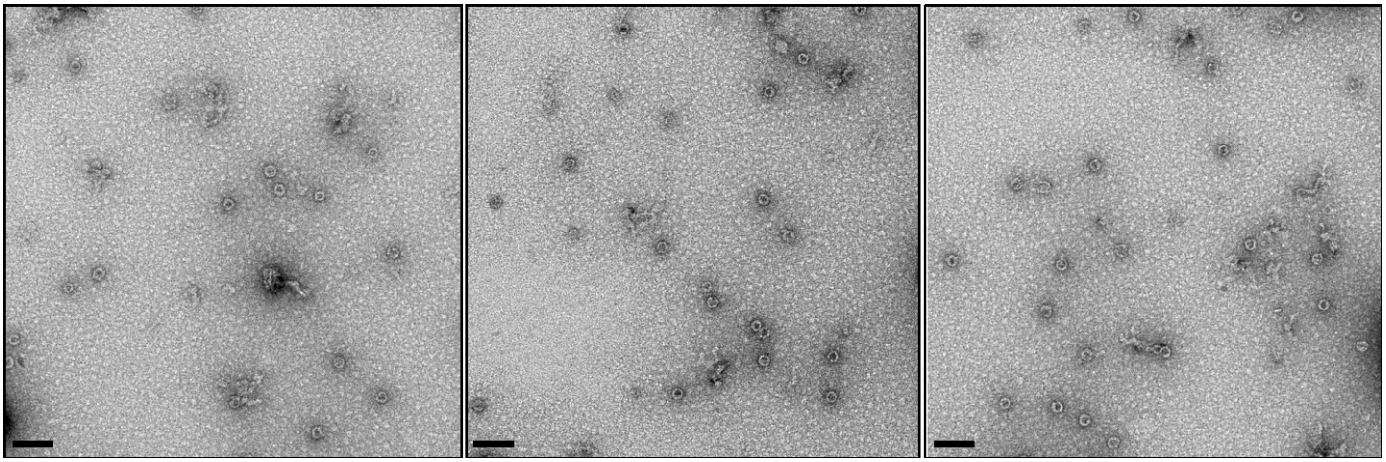

Figure S7. TEM analysis of *in vitro* assembled Halo shells. Scale bars = 100 nm.

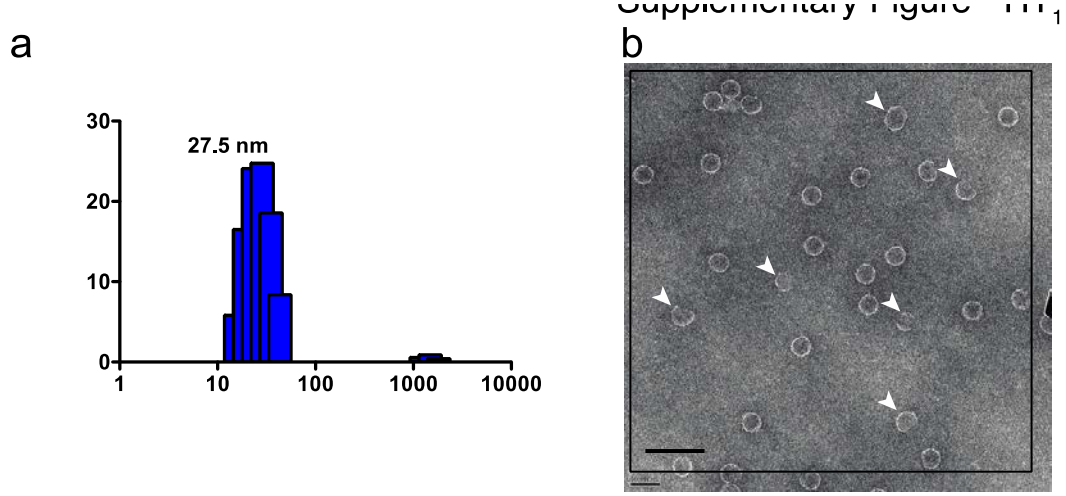

Figure S8. Structural characterization of CAP-purified *in vitro* assembled minimal HO shells. (a) Dynamic light scattering analysis plot of the mHO eluate shown in Figure 4a, lane 3. The hydrodynamic radius of the shells is labeled on the plot. The x-axis is logarithmically spaced. (b) TEM analysis of mHO shells. "Broken shell" phenotype indicated by white arrows. Scale bar = 100 nm.

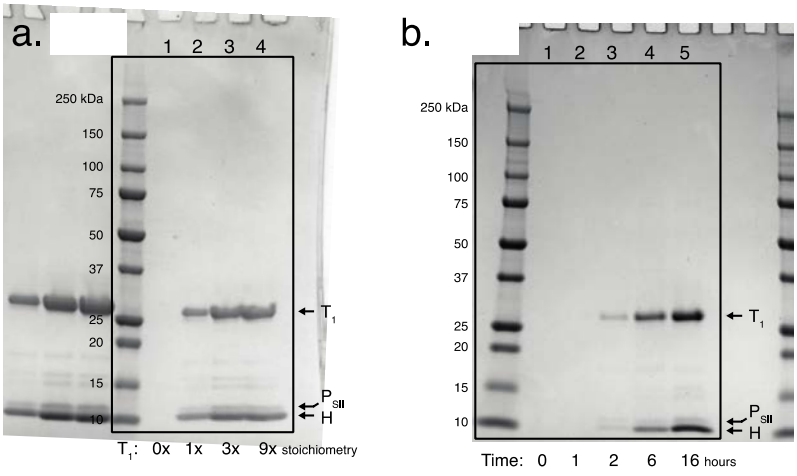

Figure S9. Uncropped SDS-PAGE gels of Figure 4 from main text. (a) Figure 4b**.** (b) Figure 4c.

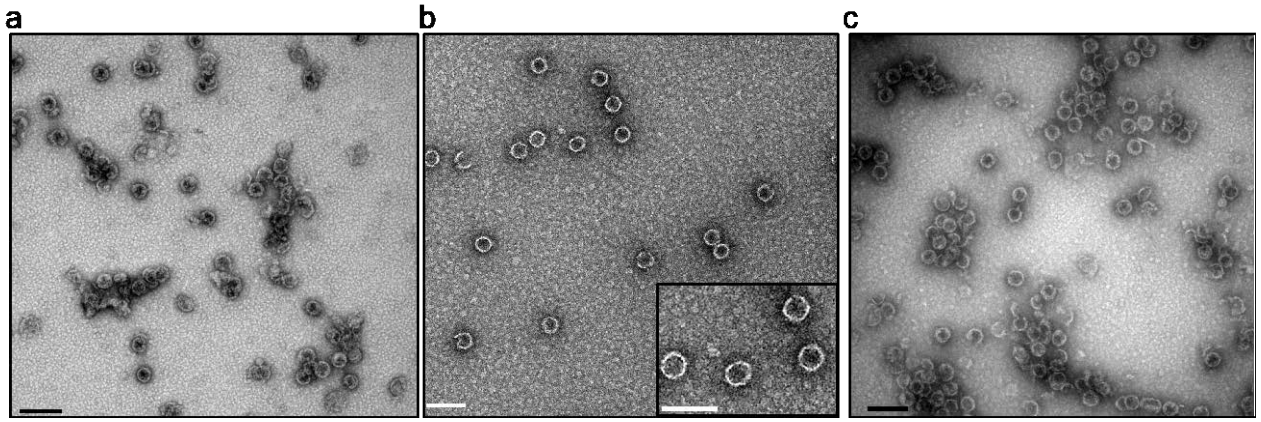

Figure S10. Representative TEM images of purified *in vitro* assembled mHO shells. (a) mHO^+ only. (b) mHO + RraB-GFP. Inset is an enlarged view of the shells (scale bar = 50 nm). (c) mHO^+ + GFP. Scale bars = 100 nm.

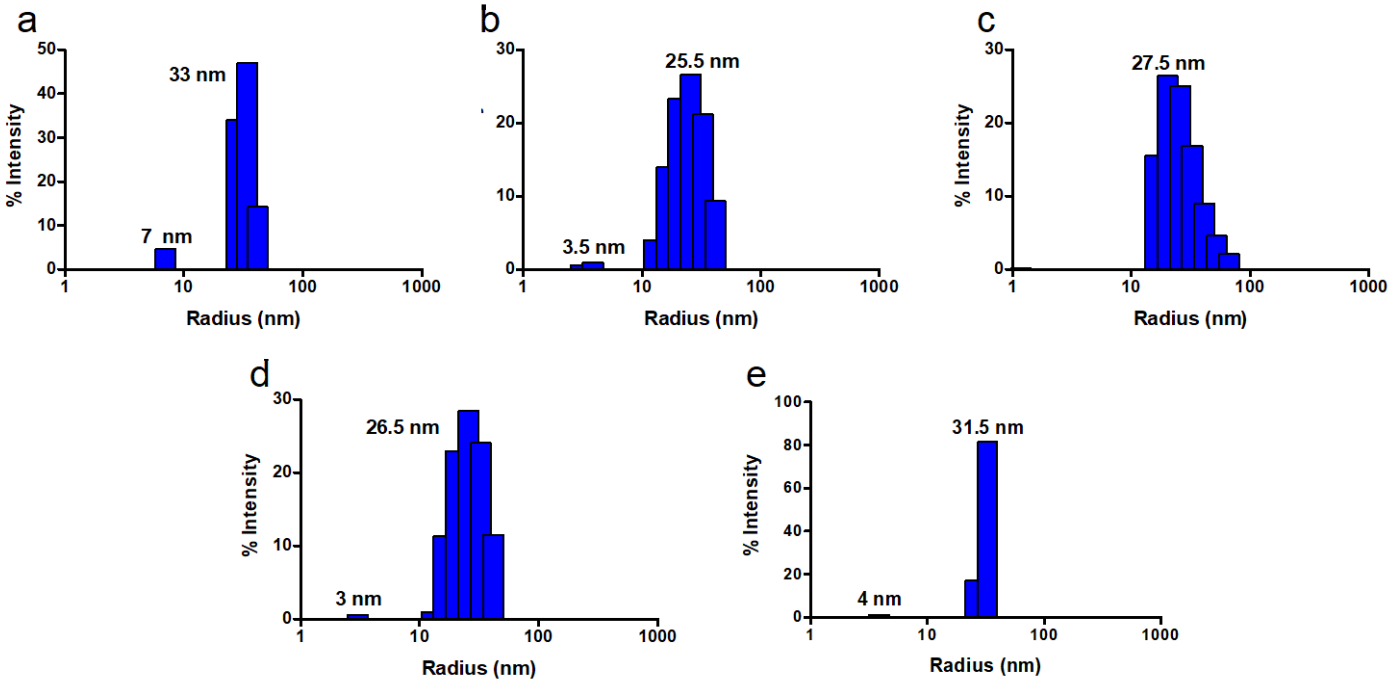

Figure S11 DLS histograms of various purified *in vitro* assembled mHO shells. (a) mHO^+ only. (b) mHO + RraB-GFP. (c) mHO^+ + RraB-GFP. (d) mHO + GFP. (e) mHO^+ + GFP. The hydrodynamic radius of the shells and other minor species is labeled on the plot. The x-axis is logarithmically spaced.

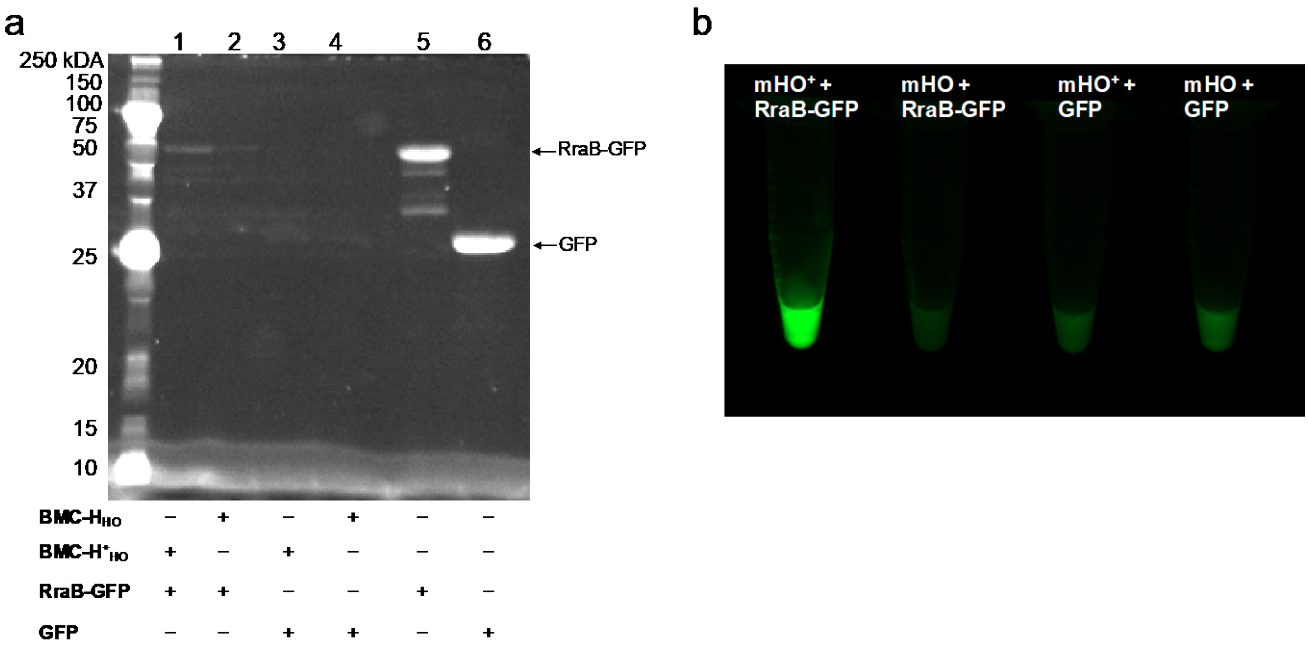

Figure S12. (a) In gel GFP fluorescence of purified mHO shell assemblies with GFP under reducing conditions. The SDS-PAGE gel was excited with blue light, and the emission from GFP measured. Lane 1 = mHO^+ + Rrab-GFP, lane 2 = mHO + RraB-GFP, lane 3 = mHO^+ + GFP, lane 4 = mHO + GFP, lane 5 = RraB-GFP, and lane 6 = GFP. Similar protein content was loaded in lanes 1-4, 1.2 – 1.9 μg. (b) Photograph of purified *in vitro* assembled mHO shells with GFP excited by a UV-transilluminator. The pooled eluates contained 0.15 – 0.46 mg/mL total protein content.

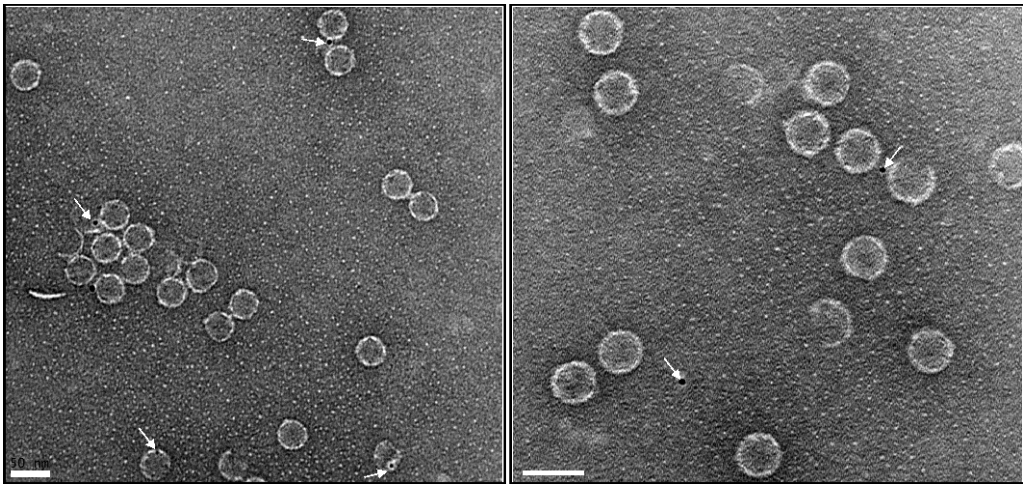

Figure S13. TEM analysis of mHO copurified with 5 nm AuCOOH particles. Left panel is a representative TEM image and right panel is an additional TEM image at a higher magnification, 200kx (white arrows point at AuCOOH particles). Scale bars = 50 nm.

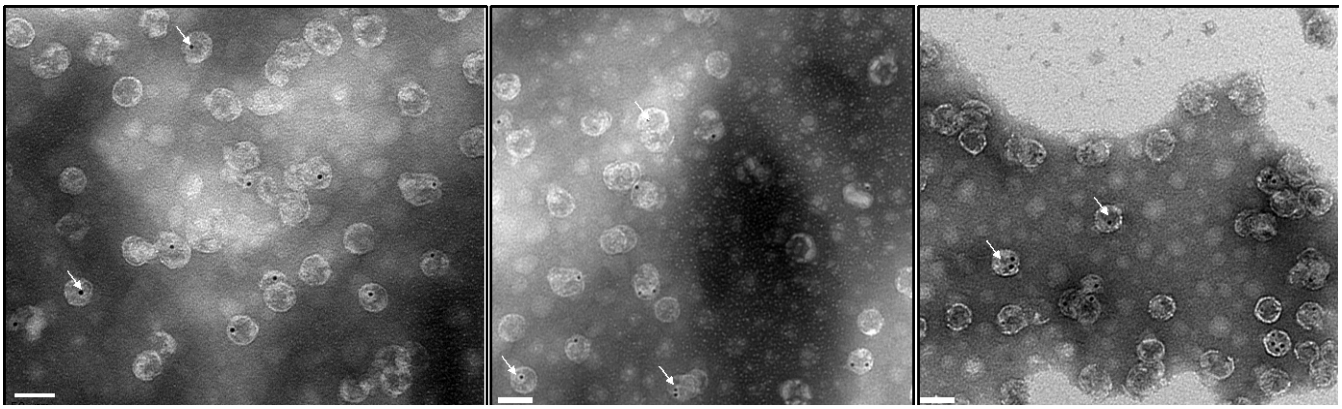

Figure S14. Representative TEM images of mHO$^+$ copurified with 5 nm AuCOOH particles. Magnification of 140 kx (white arrows point at Au particles). Scale bars = 50 nm.

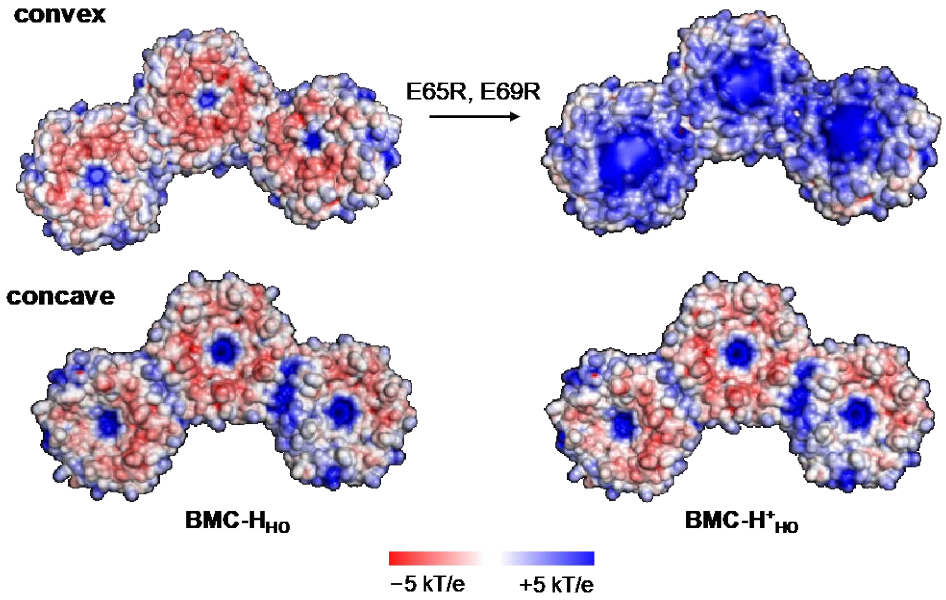

Figure S15. Charge distribution map of three hexamer. The surface colored by electrostatic potential from -5kT/e (red) and + -5kT/e (blue). The convex side orients toward the lumen, while the concave side faces the exterior of the HO BMC shell.

REFERENCES

1. Aussignargues, C.; Pandelia, M. E.; Sutter, M.; Plegaria, J. S.; Zarzycki, J.; Turmo, A.; Huang, J.; Ducat, D. C.; Hegg, E. L.; Gibney, B. R.; Kerfeld, C. A. *J Am Chem Soc* **2016,** 138, (16), 5262-70.
2. Hagen, A.; Sutter, M.; Sloan, N.; Kerfeld, C. A. *Nat Commun* **2018,** 9, (1), 2881.
3. Kapust, R. B.; Waugh, D. S. *Protein Science* **1999,** 8, (8), 1668-1674.
4. Li, S. J.; Hochstrasser, M. *Nature* **1999,** 398, (6724), 246-51.
5. Lee, T. S.; Krupa, R. A.; Zhang, F.; Hajimorad, M.; Holtz, W. J.; Prasad, N.; Lee, S. K.; Keasling, J. D. *J Biol Eng* **2011,** 5, 12.
6. Sutter, M.; Faulkner, M.; Aussignargues, C.; Paasch, B. C.; Barrett, S.; Kerfeld, C. A.; Liu, L. N. *Nano Lett* **2015**.
7. Zhou, L.; Zhao, M.; Wolf, R. Z.; Graham, D. E.; Georgiou, G. *J Bacteriol* **2009,** 191, (21), 6665-74.
8. Zou, Z.; Cao, L.; Zhou, P.; Su, Y.; Sun, Y.; Li, W. *J Biotechnol* **2008,** 135, (4), 333-9.

9. Pedelacq, J. D.; Cabantous, S.; Tran, T.; Terwilliger, T. C.; Waldo, G. S. *Nat Biotechnol* **2006,** 24, (1), 79-88.